To appear in the Astrophysical Journal.
Preprint typeset using LaTeX style emulateapj

RADIO OBSERVATIONS OF SN 1979C: EVIDENCE FOR RAPID PRESUPERNOVA EVOLUTION

Marcos J. Montes
Naval Research Laboratory, Code 7212, Washington, DC 20375-5320; montes@rsd.nrl.navy.mil
Kurt W. Weiler
Naval Research Laboratory, Code 7214, Washington, DC 20375-5320; weiler@rsd.nrl.navy.mil
Schuyler D. Van Dyk
IPAC/Caltech, Mail Code 100-22, Pasadena, CA 91125; vandyk@ipac.caltech.edu
Nino Panagia[1]
Space Telescope Science Institute, 3700 San Martin Drive, Baltimore, MD 21218; panagia@stsci.edu
Christina K. Lacey
Naval Research Laboratory, Code 7214, Washington, DC 20375-5320; lacey@rsd.nrl.navy.mil
Richard A. Sramek
P.O. Box 0, National Radio Astronomy Observatory, Socorro, NM 87801; dsramek@nrao.edu
and
Richard Park[2]
Thomas Jefferson High School for Science and Technology, Alexandria, VA; rpark@mit.edu

To appear in the Astrophysical Journal.

ABSTRACT

We present new radio observations of the supernova SN 1979C made with the VLA at 20, 6, 3.6, and 2 cm from 1991 July to 1998 October, which extend our previously published observations (Weiler et al. 1986, 1991), beginning 8 days after optical maximum in 1979 April and continuing through 1990 December. We find that the radio emission from SN 1979C has stopped declining in flux density in the manner described by Weiler et al. (1992), and has apparently entered a new stage of evolution. The observed "flattening," or possible brightening, of the radio light curves for SN 1979C is interpreted as due to the SN shock wave entering a denser region of material near the progenitor star and may be indicative of complex structure in the circumstellar medium established by the stellar wind from the red supergiant (RSG) progenitor.

Subject headings: stars — stars: evolution — supernovae: individual (SN 1979C)

1. INTRODUCTION

The study of supernovae (SNe) which are significant sources of radio emission, known as "radio supernovae" (RSNe), provides unique information on the properties of the progenitor stellar systems and their immediate circumstellar environments. In particular, changes in the density of the presupernova stellar wind established circumstellar material (CSM) alter the intensity of the radio emission and allow us to probe the mass-loss history of the supernova's progenitor, structures in the CSM, and the nature and evolution of the SN progenitor.

Significant deviation of the radio emission of SNe from standard models has previously been noted and interpreted as due to a complex CSM density structure. SN 1979C (Weiler et al. 1986, 1991) has shown a quasi-periodic variation in its radio emission which may be due to modulation of the CSM density by a binary companion (Weiler et al. 1992; Schwartz & Pringle 1996). SN 1987A, after an initial, faint radio outburst and rapid decline until 1990 June, is now increasing in radio flux density due to the SN shock starting to impinge on the inner edges of the well known, much higher density central ring (Turtle et al. 1990; Staveley-Smith et al. 1992, 1993, 1995; Ball et al. 1995; Gaensler et al. 1997). SN 1980K (Montes et al. 1998) at an age of ~ 10 years has experienced a sharp drop in its radio emission far beyond that expected from models of its previous evolution. More recently, SN 1988Z has also shown a sharp drop in its radio emission similar to that of SN 1980K (Lacey et al. 1999).

Recent observations of SN 1979C imply that the shock from SN 1979C has entered a new, higher density CSM structure different from the modulated decline previously reported (Weiler et al. 1992). The radio emission has apparently stopped declining and has been constant, or perhaps increasing, for the past eight years.

We have monitored SN 1979C [RA(2000.0) = $12^{\rm h}22^{\rm m}58\overset{\rm s}{.}67 \pm 0\overset{\rm s}{.}01$; DEC(2000.0) = $+15°47'51\overset{''}{.}8 \pm 0\overset{''}{.}2$] in NGC 4321 (M 100) since 1979 April 27, and the results through December 1990 are available in Weiler et al. (1986, 1991, 1992). Here we present new Very Large Array[3] (VLA) radio measurements between 1991 July 28 and 1998 October 19.

[1]Affiliated with the Astrophysics Division, Space Science Department of ESA.

[2]Now at the Massachusetts Institute of Technology.

[3]The VLA is operated by the National Radio Astronomy Observatory of the Associated Universities, Inc., under a cooperative agreement with the National Science Foundation.

2. OBSERVATIONS

Routine monitoring observations of SN 1979C have been carried out with the VLA at 20 cm (1.465 GHz) and 6 cm (4.885 GHz) a few times a year since 1991. On 1996 December 21 & 1998 February 10, observations were additionally made at 3.6 cm (8.435 GHz) and 2 cm (14.965 GHz). The techniques of observation, editing, calibration, and error estimation are described in previous publications on the radio emission from SNe (see, e.g., Weiler et al. 1986), with particular reference to SN 1979C in Weiler et al. (1991, 1992). The "primary" calibrator remains 3C 286 and is assumed to be constant in time with flux densities 14.45, 7.42, 5.20, and 3.45 Jy, at 20, 6, 3.6, and 2 cm, respectively. The "secondary" calibrator, 1252+119, was used as the phase (position) calibrator with a defined position of RA(1950)=$12^{\rm h}52^{\rm m}07\overset{\rm s}{.}724$, DEC(1950)= $+11^\circ57'20\overset{''}{.}82$, and, after calibration by 3C 286, as the actual flux density reference for the observations of SN 1979C. As expected for a "secondary" calibrator[4], the flux density of 1252+119 has been varying over the years, as can be seen in both Table 1 and Figure 1.

The flux density measurement error is a combination of the rms map error, which measures the contribution of small unresolved fluctuations in the background emission and random map fluctuations due to receiver noise, and a basic fractional error ϵ included to account for the normal inaccuracy of VLA flux density calibration (see, for example, Weiler et al. 1986) and possible deviations of the primary calibrator from an absolute flux density scale. The final errors (σ_f) as listed in Table 2 are taken as

$$\sigma_f^2 \equiv (\epsilon S_0)^2 + \sigma_0^2 \qquad (1)$$

where S_0 is the measured flux density, σ_0 is the map rms for each observation, and $\epsilon = 0.05$ for 20, 6, and 3.6 cm, and $\epsilon = 0.075$ for 2 cm.

3. RESULTS

Table 2 shows the new flux density measurements from 1991 July 28 through 1998 October 19, while Figure 2 shows a plot of all the available 20 and 6 cm data for SN 1979C from 1979 April 27 through 1998 October 19, along with the best-fit model through 1990 December (day $\sim$ 4,300; Weiler et al. 1992). Figure 3 shows the evolution of the spectral index between 20 and 6 cm, α_6^{20}, for all the available data through 1998 October 19, and Figure 4 shows the spectrum at four frequencies for the 1996 December 21, 1998 February 10, and February 13 observations.

The solid line in Figure 3 is calculated from the best-fit model to the data through 1990 December and is not adjusted for the change in evolution since that time. The solid line in Figure 4 is calculated for the best-fit spectrum using only data from the 1996 December 21, 1998 February 10, and February 13 observations, and may be represented as $S_\nu \propto \nu^\alpha$ with $\alpha = -0.63 \pm 0.03$. This spectral index value is clearly flatter than both the best-fit spectral index after day 4,300, $\alpha_{t>4{,}300} \sim -0.70$, and the pre-1991 best-fit spectral index of -0.75 (see Table 3). Even though for the new measurements since 1990 December α_6^{20} ranges from about $-1 \lesssim \alpha_6^{20} \lesssim -0.6$ (Figure 3), the spectral index retains a completely optically thin, nonthermal character, at least over the wavelength range from 20 to 2 cm (Figure 4). It is apparent that, while the evolution of the radio emission (and presumably the density structure of the CSM) has changed significantly since 1990 December, the best-fit spectral index, since becoming optically thin, has remained fairly constant with $\alpha_{t<4{,}300} \sim -0.75$ (before day 4,300; Figure 3) and $\alpha_{t>4{,}300} \sim -0.70$ (after day 4,300), although short-term deviations such as that seen in Figure 3 ($\alpha = -0.63$) appear to be real.

The fluctuations seen in Figure 2 in the 6 cm data (relative to the fairly constant 20 cm data) after day $\sim$ 4,300 also appear to be real. This data was reduced independently by three (and in some cases four) of the authors, all with similar results. The fluctuations are not correlated with fluctuations in the secondary calibrator 1252+119 or VLA array configuration. Higher frequency observations which would assist in the interpretation of this data are, unfortunately, available on only two dates (1996 December 21 & 1998 February 13) and have no long-term monitoring values with which to compare.

4. PARAMETERIZED MODEL

Previous work on RSNe (see, e.g., Weiler et al. 1986, 1991) has shown that the radio emission can be reasonably well described in its gross properties by a parameterized model of the form

$$S(\mathrm{mJy}) = K_1 \Big(\frac{\nu}{5\ \mathrm{GHz}}\Big)^\alpha \Big(\frac{t-t_0}{1\ \mathrm{day}}\Big)^\beta e^{-\tau}\ , \qquad (2)$$

where

$$\tau = K_2 \Big(\frac{\nu}{5\ \mathrm{GHz}}\Big)^{-2.1} \Big(\frac{t-t_0}{1\ \mathrm{day}}\Big)^\delta \qquad (3)$$

where K_1 and K_2 correspond formally to the flux density (in mJy) and uniform absorption, respectively, at 5 GHz one day after the explosion date, t_0; α is the nonthermal spectral index of the synchrotron emission; and β is the decline rate of the radio emission after maximum. The term $e^{-\tau}$ describes the attenuation of a local, external medium that uniformly covers the emitting source ("uniform external absorption") and is assumed to be purely thermal, ionized hydrogen with frequency dependence $\nu^{-2.1}$. From the Chevalier (1982a,b) model for radio emission from SNe, this CSM is assumed to have radial density dependence $\rho \propto r^{-2}$ and to have been established by a constant mass-loss rate, $\dot{M}$, constant speed wind, w, from a red supergiant progenitor. The parameter δ describes the time dependence of the optical depth for this local, uniform medium, and $\delta \equiv \alpha - \beta - 3$ is specified in the Chevalier model (Chevalier 1984). For an undecelerated SN shock, $\delta = -3$ is appropriate (Chevalier 1982a).

Chevalier (1982a) also determined the dependence of the radio luminosity on the mass-loss rate ($\dot{M}$) and progenitor wind velocity (w) or, equivalently, to the average CSM

[4]Secondary calibrators are chosen to be compact and unresolved by the longest VLA baselines. Such compact objects are usually extragalactic and variable so that their flux density must be recalibrated from the primary calibrators for each observing session.

density ($\rho_{\rm CSM} \propto \dot{M}/w$), as

$$L \propto \left(\frac{\dot{M}}{w}\right)^{(\gamma-7+12m)/4} , \quad (4)$$

where $\gamma = -2\alpha + 1$ is the power law of the relativistic electron energy distribution and $m = -\delta/3$ describes the time dependence of the self-similar evolution of the shock radius, $R \propto t^m$. In this model, the magnetic energy density and the relativistic energy density both scale as the total post-shock energy density ($\propto \rho_{\rm CSM} V_{\rm shock}^2$ where $V_{\rm shock} = dR/dt$), and both the magnetic field amplification efficiency and the particle acceleration efficiency remain constant as the SN evolves.

Weiler et al. (1992) noted periodic features in the radio light curves of SN 1979C. Since the spectral index was not affected by the observed flux density oscillations, they concluded that the variations were due to emission efficiency changes caused by modulations in the CSM density structure, rather than being due to optical depth effects. They, therefore, introduced a modification to Equation 2 by multiplying the emission term K_1 by the sinusoidally-varying modulation

$$\left\{1 + A\sin\left[2\pi B\left(\frac{t-t_0}{1\ \rm day}\right) + C\right]\right\}^{-(\alpha+2\delta+3)/2} . \quad (5)$$

Since a radial density modulation of the CSM will also affect the optical depth τ ($\tau \propto \rho_{\rm CSM}^2 \propto (\dot{M}/w)^2$), Equation 3 was modified by multiplying the absorption term K_2 by

$$\left\{1 + A\sin\left[2\pi B\left(\frac{t-t_0}{1\ \rm day}\right) + C\right]\right\}^{2} . \quad (6)$$

In Equations 5 and 6, the expression

$$A\sin\left[2\pi B\left(\frac{t-t_0}{1\ \rm day}\right) + C\right] \quad (7)$$

represents the deviation of $\dot{M}/w$ from a constant pre-SN wind mass-loss rate[5]. The parameters A, B, and C define the sinusoidal variation of $\rho_{\rm CSM}$ ($\propto \dot{M}/w$), where A represents the fractional amplitude of the density modulation, B represents its frequency (in cycles day^{-1}), and C represents its phase lag (in radians).

The best-fit model parameters to the pre-1991 ($t - t_0 <$ 4,300 days) data are listed in Table 3. This fit is slightly different from that of Weiler et al. (1992), due to improved fitting software, but agrees with that work to within the uncertainties. The errors in these new fitting parameters were estimated using a bootstrap procedure (Press et al. 1992). Bootstrap procedures use the actual data sets to generate thousands of synthetic data sets that have the same number of data points, but some fraction of the data is replaced by duplicated original points. The fitting parameters are then estimated for these synthetic data sets using the same algorithms that are used to determine the parameters from the actual data. The ensemble of parameter fits is then used to estimate errors for the parameters by examining number distributions for the parameter in question. The errors in the fitting parameters in Table 3 correspond to the values with 15.85% and 84.15% (i.e., $\pm 1\sigma$ for a Gaussian distribution), respectively, of the cumulative distribution for each parameter.

5. DISCUSSION

5.1. *Interpretation*

As can be seen in Figure 2, the new measurements for SN 1979C since 1991 July 28 do not fit the model which described the data relatively well through 1990 December. Since that time, the flux densities at all frequencies appear to have stopped declining and perhaps even started increasing. Accepting our previous interpretation that a constant spectral index indicates an unchanged emission mechanism with constant efficiencies, this flattening implies that the shock wave of the SN is now interacting with a higher density structure in the CSM.

Under this scenario, the flattening of the radio light curve may imply either the presence of denser circumstellar material (§5.2.1), or perhaps a geometrical solution, such as the presence of a flared disc or ring (§5.2.2). Such dense shells or rings, similar to those we propose, are present around early type stars, as indicated by observations of luminous blue variable (LBV) stars (see, e.g., Nota et al. 1995), the recent detections of rings around B type supergiants (see, e.g., Brandner et al. 1997), and even by SN 1987A with its prominent circumstellar ring.

Another example of a SN surrounded by a circumstellar shell denser than a normal RSG wind is provided by SN 1978K, for which Montes et al. (1997) have found evidence of a constant free-free absorption that produces a characteristic low-frequency curvature in the typical synchrotron radio spectrum of the SN. The presence of a discrete shell of ionized gas surrounding SN 1978K has been confirmed by Chu et al. (1999) through spectroscopic measurements showing narrow Hα and [N II] emission lines with widths and intensities characteristic of the environment around LBV stars.

Additionally, there is evidence from optical observations of SN 1979C that the Hα and [O I] emission lines are also not decreasing, but have remained flat or perhaps increased slightly (Fesen et al. 1999). The optical emission arises from a different emission mechanism than the radio emission and at a different region of the SN shock, providing a separate line of evidence that SN 1979C has encountered a higher density region of the circumstellar medium.

Furthermore, recent results from simulations of young SNRs interacting with higher density clouds of varying sizes in an otherwise uniform CSM (Jun & Jones 1999 and references therein) have shown that radio emission increases due to the increased ambient density and turbulent magnetic field amplification after a SNR/cloud interaction begins. The simulations also showed changes in the efficiencies over time arising from the SNR/cloud interaction,

[5]While it is true that the optical depth is due to the *integral* along the line of sight to the radio emitting region, most of the absorption occurs close to the shock front where the density is the greatest. The fractional errors in τ from using our equations (3) and (6) instead of the actual integrated expression for τ vary roughly sinusoidally with a period $\sim 1/B$, and a magnitude $\sim 2A$. At the epoch we are concerned with, $\tau \ll 1$, thus the fractional errors in $e^{-\tau}$ are much smaller than $2A$.

and how, in such interactions, the efficiencies, magnetic fields, and densities do not scale in the simple manner described by the Chevalier (1982a,b) model.

However, it must be noted that a change in the observed radio emission could be caused by a change in the efficiency of particle acceleration without significant CSM density change. Since the efficiency of particle acceleration is not well understood, an efficiency change may or may not cause a noticeable change in the spectral index. If we take the η to be the ratio between the number of electrons that are accelerated to the total number of electrons, then η is linearly proportional to the measured flux density. While we may not know η, we do know that the ratio of the measured flux density to that expected from the Chevalier model. If we assume that *only* η changes, while the densities and magnetic fields behave as expected from the Chevalier model, then $\eta_{7100\ \mathrm{days}}/\eta_{4300\ \mathrm{days}} = S_{\mathrm{measured}}/S_{\mathrm{model}} \sim 1.7$. This would require that the acceleration efficiency had remained roughly constant until $\sim$ 4,300 days after explosion, then continually increase, being some $\sim$ 70% greater by day $\sim$ 7,100 than at day $\sim$ 4,300. Nevertheless, given the optical evidence of an increase in the circumstellar density, which does not rely on particle acceleration, we interpret the deviation of the radio emission of SN 1979C from the previously assumed model as due to local density enhancement with the particle acceleration efficiency relatively unchanged.

5.2. *Nature of the Necessary Density Enhancement*

5.2.1. *CSM Density Increase*

A denser CSM may either be an isotropic shell or be in the form of condensations which have a small combined covering factor $\phi = \Omega/4\pi < 1$, relative to the expanding shock front which is overtaking them. Since the flux density increase at $t \simeq$ 7,100 days is about a factor of 1.7 greater than that expected from the previous best-fit model (Weiler et al. 1991), and since the radio luminosity has a power-law dependence on the CSM density ($L_{\mathrm{radio}} \propto \rho_{\mathrm{CSM}}^{1.82}$, Chevalier 1982a), the implied density enhancement is a factor of $\sim 1.34\phi^{-0.55}$ greater than the expected density for a $\rho \propto r^{-2}$ constant mass-loss rate, constant velocity wind established CSM. Moreover, the increase relative to the best-fit model behavior is gradual with time, indicating a relatively smooth density distribution, which decreases with radius more slowly than the expected r^{-2} behavior. To produce an increase of density by a factor $\sim$ 1.34 between 4,300 and 7,100 days a new radial density profile of approximately $\rho_{\mathrm{CSM}} \propto r^{-1.4}$ is required if $\phi = 1$, i.e., for a uniform density distribution.

If the density enhancement is the result of discrete features, whether a shell, condensations, or a ring, it is likely to fill a relatively limited fraction of the space around the SN progenitor, and to be present over a limited interval of radii ($\Delta R/R < 1$). Thus, this increase of radio emission could be a transient phase that disappears in a relatively short time.

The argument for a limited duration to the increased radio emission, at least for a spherical geometry, is based on the plausible initial mass of the SN's RSG progenitor. The best-fit parameters for the radio emission at $t <$ 4,300 days (Table 3) imply a pre-SN mass-loss rate of $\dot{M} \simeq 1.6 \times 10^{-4}\ M_\odot\ \mathrm{yr}^{-1}$, if one adopts a pre-SN stellar wind velocity of 10 km s^{-1}, a shock velocity of 9,250 km s^{-1} (Bartel 1991), and an electron temperature (T_e) of 30,000 K for the CSM. At a SN shock velocity of $9,250$ km s^{-1}, by 4,300 days after the explosion the front has reached a distance in the pre-SN wind, with assumed velocity 10 km s^{-1}, where the material was lost from the star $\sim$ 11,000 years before the explosion. At such a mass-loss rate ($\dot{M}$) and wind velocity (w) the CSM, through which the shock has already passed, amounts to $\sim 1.7M_\odot$, a significant amount of material, even from a massive progenitor star. The additional matter present in the next layers, i.e. between 4,300 and 7,100 days, corresponds to another $\sim 2.2M_\odot$, making a total mass $\sim$ 3.9 $M_\odot$ of swept-up CSM by 1998 October. If the flux density continues to evolve in the present manner, the amount of engulfed matter increases rapidly: for example, in another 8 years (i.e., by the year 2007) the additional swept mass would be $\sim 2.9M_\odot$, giving a total swept-up mass of $\sim 6.8\ M_\odot$.

Such a swept wind mass is large, even for a red supergiant star, and it implies a very massive progenitor. Estimates of the mass of the envelope ejected by SN 1979C range from $M_{\mathrm{env}} \sim 1M_\odot$ (Chugai 1985) to $M_{\mathrm{env}} \sim 6M_\odot$ (Branch et al. 1981; Bartunov & Blinnikov 1992; Blinnikov & Bartunov 1993). In particular, in the models by Bartunov & Blinnikov (1992) for SN 1979C, the CSM has a reasonable density profile, matching the observed B light curves of SN 1979C quite well. Adopting their value for M_{env}, assuming a stellar remnant mass of $M_{\mathrm{rem}} \sim 1.4M_\odot$, and using our above estimate for the current value of the swept-up mass, the initial mass of the progenitor must have been $M_0 \gtrsim 11.3M_\odot$. Assuming the current evolution of the flux density continues, by 2007 our estimate would rise to $M_0 \gtrsim 14.2M_\odot$. While large, this is still consistent with the estimates of Van Dyk et al. (1999). From their HST imaging of the SN 1979C environment, they find that the stellar ages in that environment are consistent with the SN progenitor having an initial mass of $M_0 \approx 17$–$18M_\odot$.

5.2.2. *Equatorial wind or disc*

Alternatively, the increase in flux density could be an effect of the geometry of the CSM. It is conceivable that at small radii the CSM was distributed in a disk with constant solid angle. At a radius of $\sim 3.4 \times 10^{17}$ cm (0.11 pc, the radius reached by a 9,250 km s^{-1} shock after 4,300 days) the disk thickness increases so that it covers a larger solid angle, reaching about twice the initial solid angle by day 7,100 while maintaining a $\rho \propto r^{-2}$ behavior. Such a flared geometry would ease the mass requirement if the original disk subtended a relatively small angle (Ω) and is at a large inclination angle, so as to be seen almost edge-on. In such a case the mass-loss rate determined by radio light curve fitting (in which the rate is derived essentially from the free-free absorption of the CSM) would only be valid within the solid angle subtended by the disk, rather than over the full 4π steradians. Then, the mass engulfed by day 4,300 would be reduced by a factor $\Omega/4\pi$ and could be as small as $\sim 1/10$ of the estimates in the previous section, without making the requirement on the viewing inclination angle too severe. However, even in such a case, the flux density flattening observed since day 4,300 requires

an increase of the interacting surface, so that the mass engulfed at later times increases at the same rate as the flux density does relative to the best-fit model. For example, if we take an initial solid angle of the disk to be $\Omega = 4\pi/3$, the mass swept by day 4,300 would be $\sim 0.57\ M_\odot$ and the mass swept-up by day 7,100 would be an additional $\sim 0.54\ M_\odot$. More generally, if we denote with ϕ the fraction of solid angle subtended by the disk in the inner region, the mass swept by day 4,300 would be $1.71\phi\ M_\odot$ and the mass subsequently swept up by day 7,100 would be $\sim 1.44\phi M_\odot$, a large, but much smaller amount than for the spherical shell case.

5.2.3. *Model discrimination*

A possible discriminant between the two basic possibilities, an increase of CSM density or an increase of CSM coverage, is the measurement of free-free absorption at low frequencies. For the case of flattening flux density due to a less rapidly declining (as $\rho \propto r^{-1.4}$ rather than $\rho \propto r^{-2}$) CSM density the emission measure will begin to decrease as EM $\propto r^{-1.8}$, while for the case of flattening flux density due to increasing coverage factor, the emission measure behavior will be either the same as, or steeper than the canonical stellar wind $\rho \propto r^{-2}$ and could vary as much as EM $\propto r^{-3}$ or more. In temporal terms, the differing density dependence of the EM implies that up to 4,300 days the emission measure decreased as EM$\propto t^{-3}$, and that for $t - t_0 >$ 4,300 days its behavior changed to EM$\propto t^{-1.8}$. However, this behavior can only be tested at those frequencies where the optical depth was of the order of unity at 4,300 days, so that observations at lower frequencies than the 1.4 GHz will be required to distinguish between the two scenarios.

To estimate how low an observing frequency is required to see the difference, the best-fit model gives an optical depth of

$$\tau(\nu) = 1.45 \left(\frac{t}{\text{1,000 days}}\right)^{-3} \left(\frac{\nu}{\text{1 GHz}}\right)^{-2.1} , \qquad (8)$$

so that at 4,300 days the free-free optical depth was of the order of unity at 148 MHz and ~ 0.3 at 250 MHz. Even 330 MHz observations at the VLA are insufficient as they would probe an optical depth of only ~ 0.2 at day 4,300. Thus, testing these models may be impractical, since no high resolution, high sensitivity radio telescopes currently exist at such low frequencies.

5.3. *The Possibility of a Clumpy CSM*

We have previously postulated that the CSM around SN 1979C is highly structured (Weiler et al. 1991, 1992), and we and others have found evidence for a clumpy CSM in SN 1986J (Weiler et al. 1990) and SN 1988Z (Van Dyk et al. 1993; Chugai & Danziger 1994). We may also speculate that there is evidence for a dense clumpy medium surrounding SN 1979C from the fact that the 1.4 GHz flux densities at $t >$ 4,300 days remain relatively constant and consistently higher than predictions from the best-fit model, while the 5 GHz flux density values fluctuate from as low as the best-fit model extrapolation, to as high as 0.47 times the 1.4 GHz flux densities, with a range of spectral indices from about $-1 \lesssim \alpha_6^{20} \lesssim -0.6$ (as shown in Figure 3). These fluctuations appear real in that they greatly exceed the estimated measurement errors and seem to have a time scale of $\lesssim 1$ year. Unfortunately, the paucity of observations in the 4,300–7,100 day interval makes it hard to test this hypothesis in detail.

If real, this 5 GHz fluctuation and 1.4 GHz stability could indicate a "cooling" time of ~ 0.5 year for the relativistic electrons responsible for the higher frequency emission and an appreciably greater time constant for lower energy electrons. This could be evidence for the presence of a relatively small number of dense clumps interspersed in the general, stellar wind-generated CSM, but requires a cooling effect which is a very strong function of frequency. Synchrotron and inverse Compton losses scale only as $\nu^{-1/2}$, and Coulomb losses as $\nu^{1/2}$ (see, for example, the analysis of SN 1993J by Fransson & Björnsson 1998), so that producing such a large variation in time scales over such a small frequency range by these mechanisms is very difficult. Additionally, in order to produce such losses at all, synchrotron cooling would require magnetic fields $H \sim 1$ G, much greater than the expected $\mathcal{O}$(1 mG) fields. Unfortunately, there are too few measurements at 8.4 and 14.96 GHz (only two at each frequency) to determine if the fluctuations are also seen at higher frequencies.

Other evidence for dense clumps comes from the estimate of high densities ($n_e > 10^6$ cm^{-3}) derived by Fesen et al. (1999) from optical and UV spectroscopy of SN 1979C. However, it is hard to assess the significance of their result, because their density estimate is based on a comparison of [O II] and [O III] line intensities measured at two epochs about 4 years apart, with the unverified assumption that the line fluxes do not change with time. Additionally, the optical emission and radio emission probably arise from different physical media, making it difficult to directly compare the densities derived by Fesen et al. (1999) with the radio results. Chugai & Danziger (1994) discriminated between equatorial disc and clump models for the case of SN 1988Z by using the intermediate velocity component of the emission lines with FWHM of $\sim$ 2,000 km s^{-1}. Fesen et al. (1999) propose that the "spiky" profiles of several lines from SN 1979C are suggestive of clumpy emission regions, and individual spikes in the profiles of [O I]λ6300 and [O II]λ7325 in their Figure 5 have roughly the same velocity width as the lines used by Chugai & Danziger (1994) for the case of SN 1988Z.

The possible presence of clumps in the CSM and the reality of high frequency fluctuations should be tested. More frequent, multi-frequency radio observations ($\sim$ every three months) at a number of frequencies $>$ 1.4 GHz might establish the nature of the apparent radio flux density fluctuations, and simultaneous optical/UV observations would permit an unambiguous determination of the gas density in the clumps. We have already begun more frequent monitoring of SN 1979C with the VLA including both higher (8.4 & 14.9 GHz) and lower (330 MHz) frequencies.

6. CONCLUSIONS

Analysis of the radio emission from the Type II RSN 1979C at 20 and 6 cm from 1991 July 28 through 1998 October 19, has shown that its radio emission has unexpectedly stopped decreasing in flux density and has flattened, or perhaps begun increasing, while maintain-

ing a relatively constant spectral index. Such behavior is in conflict with the best-fit model parameter predictions, based on an assumed $\rho \propto r^{-2}$ CSM established by a constant mass-loss rate, constant velocity wind from the pre-SN star. We interpret this "flattening" to indicate that the SN shock wave has encountered a new region of CSM which was formed by the SN's progenitor $\sim$ 10,000–15,000 years before the SN explosion.

Interpretation of the data implies that this new region could either be a higher density shell, which should soon be crossed by the fast moving shock, or a "flared" disk-like structure in the CSM, if the mass-loss were constrained to a narrow solid angle. Additionally, rapid radio flux density fluctuations at 5 GHz, which are not present at 1.4 GHz, are interpreted as possible evidence for clumps or large scale density enhancements in the CSM.

Continued monitoring of SN 1979C at multiple radio frequencies – which is ongoing– is needed to determine the form and duration of this new phase in the evolution of the radio light curves and, correspondingly, the structure of this new component of the CSM. With the longest, relatively complete, multi-frequency data set available for the emission from any supernova, SN 1979C serves as a unique laboratory for understanding of the evolution of Type II supernova progenitors, their pre-SN mass-loss history, and their interactions with their local environments.

We wish to thank the referee, Stephen Reynolds, for his helpful comments and suggestions. KWW, CKL, & MJM wish to thank the Office of Naval Research (ONR) for the 6.1 funding supporting this research. CKL additionally thanks the NRC for funding supporting this research. Richard Park was a participant in the Science and Engineering Apprenticeship (SEAP) program at the NRL and continued this work as a senior thesis project at Thomas Jefferson High School of Science and Technology. Additional information and data on RSNe can be found on `http://rsd-www.nrl.navy.mil/7214/weiler/` and linked pages.

REFERENCES

Ball, L., Campbell-Wilson, D., Crawford, D. F., & Turtle, A. J. 1995, ApJ, 453, 864
Bartel, N. 1991, in Supernovae: The Tenth Santa Cruz Summer Workshop in Astronomy and Astrophysics, ed. S. E. Woosley (New York: Springer-Verlag), p. 503
Bartunov, O. S., & Blinnikov, S. I. 1992, Pis'ma AZh, 18, 104 (SvA Lett, 18, 43)
Blinnikov, S. I., & Bartunov, O. S. 1993, A&A, 273, 106
Branch, D., Falk, S. W., McCall, M. L., Rybski, P., Uomoto, A. K., & Wills, B. J. 1981, ApJ, 244, 780
Brandner, W., Chu, Y.-H., Eisenhauer, F., Grebel, E. K., Points, S. D. 1997, ApJ, 489, L153
Chevalier, R. A. 1982a, ApJ, 259, 302
———. 1982b, ApJ, 259, L85
———. 1984, ApJ, 285, L63
Chu, Y.-H., Caulet, A., Montes, M. J., Panagia, N., Van Dyk, S. D., & Weiler, K. W. 1999, ApJ, 512, L51
Chugai, N. N. 1985, Pis'ma AZh, 11, 357 (SvA Lett, 11, 148)
Chugai, N. N., & Danziger, I. J. 1994, MNRAS, 268, 173
Fesen, R. A., Gerardy, C. L., Filippenko, A. V., Matheson, T., Chevalier, R. A., Kirshner, R. P., Schmidt, B. P., Challis, P., Fransson, C., Leibundgut, B., & Van Dyk, S. D. 1999, ApJ, 117, 125
Fransson, C., & Björnsson, C.-I. 1998, ApJ, 509, 861
Gaensler, B. M., Manchester, R. N., Staveley-Smith, L., Tzioumis, A. K., Reynolds, J. E., & Kesteven, M. J. 1997, ApJ, 479, 845
Jun, B.-I. & Jones, T. W. 1999, ApJ, 511, 774
Lacey, C. K., Weiler, K. W., Van Dyk, S. D., & Sramek, R. A. 1999, BAAS, 194, #86.05
Montes, M. J., Weiler, K. W., & Panagia N. 1997, ApJ, 488, 792
Montes, M. J., Van Dyk, S. D., Weiler, K. W., Sramek, R. A., & Panagia, N. 1998, ApJ, 506, 874
Nota, A., Livio, M., Clampin, M., Schulte-Ladbeck, R. 1995, ApJ, 448, 788
Press, W. H., Teukolsky, S. A., Vetterling, W. T., Flannery, B. P. 1992, Numerical Recipes in Fortran (Cambridge:Cambridge University Press), p. 686
Schwartz, D. H. & Pringle, J. E. 1996, MNRAS, 282, 1018
Staveley-Smith, L., Manchester, R. N., Kesteven, M. J., Campbell-Wilson, D., Crawford, D. F., Turtle, A. J., Reynolds, J. E., Tzioumis, A. K., Killeen, N. E. B. K., & Jauncey, D. L. 1992, Nature, 355, 147
Staveley-Smith, L., Briggs, D. S., Rowe, A. C. R., Manchester, R. N., Reynolds, J. E., Tzioumis, A. K., & Kesteven, M. J. 1993, Nature, 366, 166
Staveley-Smith, L., Manchester, R. N., Tzioumis, A. K., Reynolds, J. E., & Briggs, D. S. 1995, in IAU Colloquium 145: Supernovae and Supernova Remnants, ed. R. M. McCray (Cambridge:Cambridge Univ. Press), p. 309
Turtle, A. J., Campbell-Wilson, D., Manchester, R. N., Staveley-Smith, L., & Kesteven, M. J. 1990, IAU Circ., 5086
Van Dyk, S. D., Peng, C. Y., Barth, J. A., & Filippenko, A. F. 1999, PASP, 111, 313
Van Dyk, S. D., Weiler, K. W., Sramek, R. A., & Panagia, N. 1993, ApJ, 419, L69
Weiler, K. W., Van Dyk, S. D., Pringle, J., & Panagia, N. 1992, ApJ, 399, 672
Weiler, K. W., Van Dyk, S. D., Panagia, N., Sramek, R., & Discenna, J. 1991, ApJ, 380, 161
Weiler, K. W., Panagia, N., & Sramek, R. A. 1990, ApJ, 364, 611
Weiler, K. W., Sramek, R. A., Panagia, N., van der Hulst, J. M., & Salvati, M. 1986, ApJ, 301, 790

TABLE 1
MEASURED FLUX DENSITY VALUES FOR THE SECONDARY CALIBRATOR 1252+119

Observation Date	Time Since SN 1979C Optical Max. (days)	S_{20} (Jy)	S_6 (Jy)	$S_{3.6}$ (Jy)	S_2 (Jy)
1979 Apr 19	$\equiv 0$	···	···	···	···
1991 Jul 28	4483	0.770	0.607	···	···
1991 Oct 31	4578	0.834	0.717	···	···
1992 Mar 01	4700	0.776	0.628	···	···
1992 Oct 13	4926	0.757	0.674	···	···
1993 Jan 28	5033	0.795	0.672	···	···
1993 May 07	5132	···	0.673	···	···
1993 Oct 17	5295	0.771	0.717	···	···
1994 Feb 18	5419	0.789	0.738	···	···
1994 Apr 25	5485	0.753	0.721	···	···
1995 Jun 15	5901	0.752	0.677	···	···
1995 Dec 12	6081	0.771	0.746	···	···
1996 Oct 06	6380	0.772	0.772	···	···
1996 Dec 21	6456	0.736	0.791	0.753	0.704
1997 Sep 23	6732	0.740	0.702	···	···
1998 Feb 10	6872	···	···	0.845	0.876
1998 Feb 13	6875	0.769	0.720	···	···
1998 Oct 19	7123	0.785	0.771	···	···

TABLE 2
NEW FLUX DENSITY MEASUREMENTS FOR SN 1979C[a]

Obs. Date	Time Since Optical Max.[b] (days)	VLA Conf.	Flux Density (mJy)							
			S_{20}	σ_{20}	S_6	σ_6	$S_{3.6}$	$\sigma_{3.6}$	S_2	σ_2
1979 Apr 19	$\equiv 0$	···	···	···	···	···	···	···	···	···
1991 Jul 28	4483	A	5.229	0.276	1.915	0.103	···	···	···	···
1991 Oct 31	4578	B	5.365	0.289	1.546	0.101	···	···	···	···
1992 Mar 01	4700	C	5.640	0.801	2.253	0.120	···	···	···	···
1992 Oct 13	4926	A	5.396	0.287	2.574	0.143	···	···	···	···
1993 Jan 28	5033	A	5.582	0.304	2.625	0.136	···	···	···	···
1993 May 07	5132	B	···	···	2.583	0.138	···	···	···	···
1993 Oct 17	5295	C/D	5.190	0.281	2.251	0.115	···	···	···	···
1994 Feb 18	5419	D/A	5.670	0.535	1.660	0.311	···	···	···	···
1994 Apr 25	5485	A	5.810	0.314	2.740	0.170	···	···	···	···
1995 Jun 15	5901	A	5.340	0.328	1.740	0.240	···	···	···	···
1995 Dec 12	6081	B	5.663	0.074	2.664	0.139	···	···	···	···
1996 Oct 06	6380	D/A	5.640	0.335	2.170	0.170	···	···	···	···
1996 Dec 21	6456	A	5.820	0.315	2.690	0.180	2.000	0.112	1.120	0.195
1997 Sep 23	6732	CnD	4.200	0.452	1.727	0.107	···	···	···	···
1998 Feb 10	6872	D	···	···	···	···	1.930	0.107	0.950	0.264
1998 Feb 13	6875	DnA	5.460	0.279	2.680	0.149	···	···	···	···
1998 Oct 19	7123	B	5.140	0.406	2.500	0.136	···	···	···	···

[a]For previous measurements, cf. Weiler et al. (1986, 1991).

[b]The date of the explosion is taken to be 1979 April 4, 15 days before optical maximum (cf. Weiler et al. 1986).

TABLE 3
FITTING PARAMETERS FOR SN 1979C[a]

Parameter	Value	Deviation Range[b]
K_1(mJy)	1710	1440–2060
α	-0.75	$-(0.76$–$0.63)$
β	-0.80	$-(0.83$–$0.78)$
K_2	3.38×10^7	$(2.97$–$3.82)\times 10^7$
$\delta \equiv \alpha - \beta - 3$	-2.94	$-(2.96$–$2.92)$
A	7.3×10^{-2}	$(6.7$–$8.1)\times 10^{-2}$
B^{-1}(days)	1570	1520–1610
C	0.90π	$(0.83$–$0.99)\pi$
t_0	$\equiv$1979 Apr. 4	...
χ^2/DOF	2.47	...

[a]Only data through 1990 December are used in the fitting procedure.

[b]The error estimates for the parameter values are determined using the bootstrap method, which is described in §4.

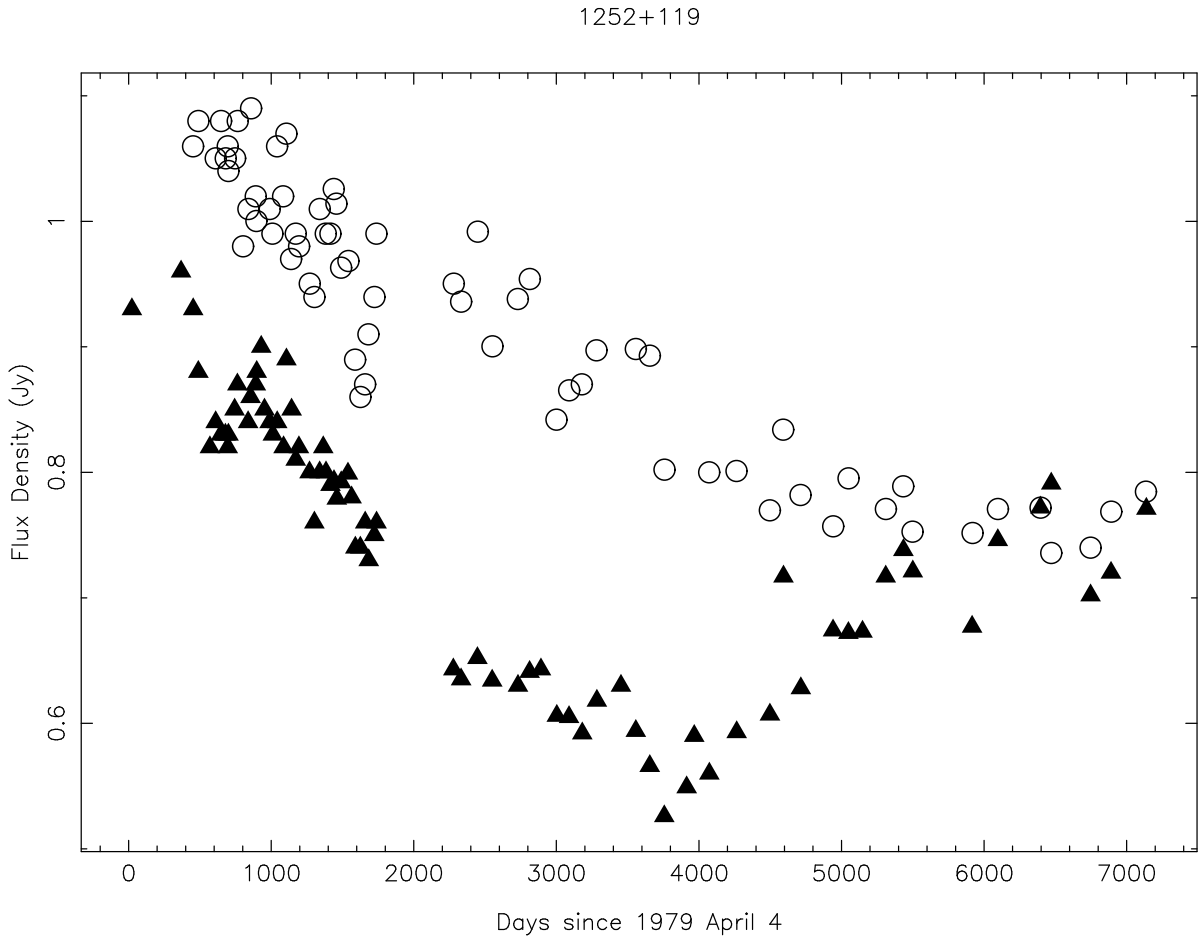

Fig. 1.— Measured flux densities for the secondary calibrator 1252+119 at 6 cm (*filled triangles*) and 20 cm (*open circles*).

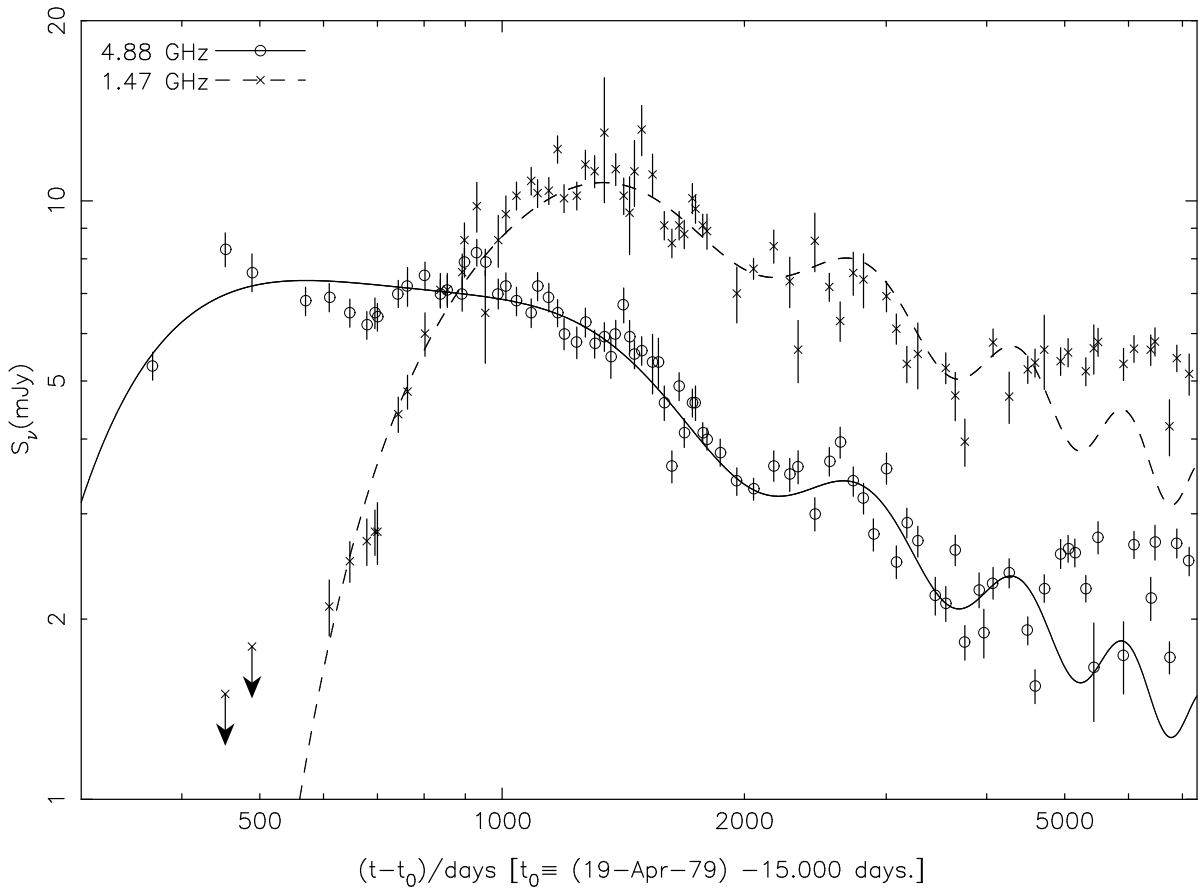

Fig. 2.— Radio "light curves" for SN 1979C in NGC 4321 (M100) at wavelengths 20 cm (*crosses*) and 6 cm (*open circles*). (Since there are only two new measurements available at 3.6 and 2 cm, they are not plotted here. However, they are shown as confirming the nonthermal nature of the spectrum in Figure 4.) The data represents about 18 years of observations for this object, including the new observations presented in this paper and previous observations from Weiler et al. (1986, 1991). The curves represent the best-fit model light curves at 6 cm (*solid*), and 20 cm (*dashed*), including the quasi-periodic, or sinusoidal, term proposed by Weiler et al. (1992). The best-fit parameters were determined using only data through 1990 December (day $\sim$ 4,300).

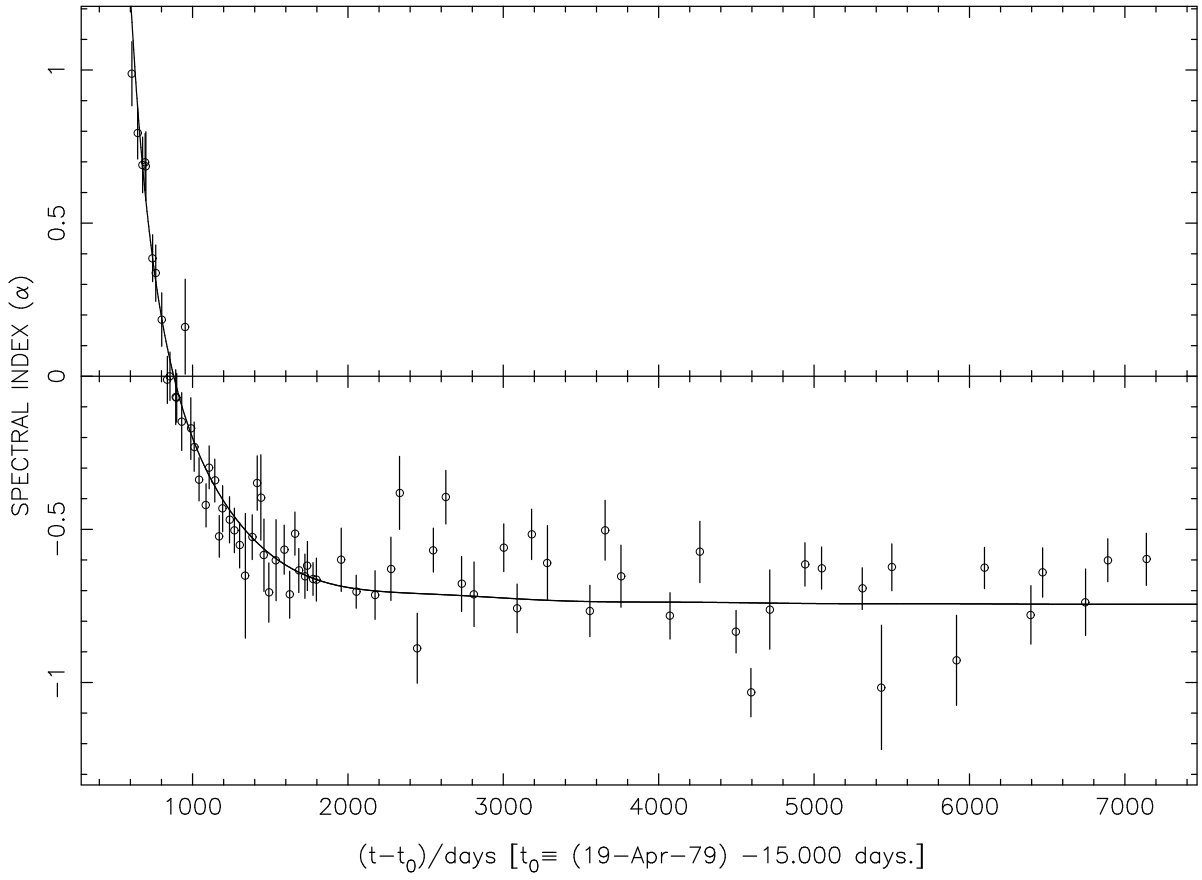

Fig. 3.— Evolution of spectral index α (where $S \propto \nu^{+\alpha}$) between 20 and 6 cm for SN 1979C, plotted as a function of time (in days) since the estimated explosion date of 1979 April 4 (15 days before optical maximum). The solid line is calculated from the best-fit theoretical "light curves" shown in Fig. 2. For reference, see Figure 3 in Weiler et al. (1986) and Figure 2 in Weiler et al. (1991).

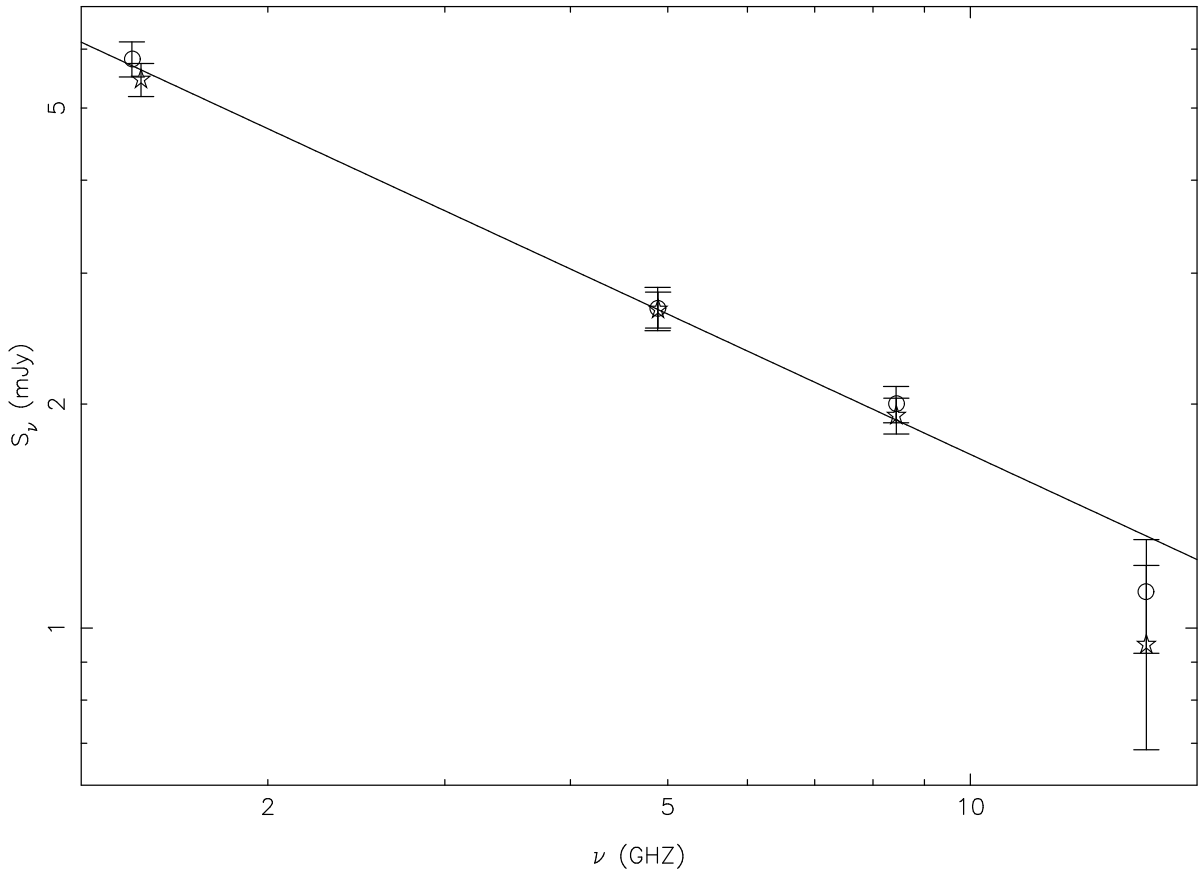

Fig. 4.— The radio spectrum for SN 1979C on 1996 December 21 (*open circles*) and 1998 February 10 & 13 (*open stars*) from 20 to 2 cm. Note that, to within the errors, the spectra are completely optically thin at all frequencies. The solid line is the best-fit spectrum to the combined data from both dates. The best-fit spectral index value for the combined data on these dates is $\alpha = -0.63 \pm 0.03$.